Biochemistry and Biophysics Reports 10 (2017) 267–275

Contents lists available at ScienceDirect

Biochemistry and Biophysics Reports

journal homepage: www.elsevier.com/locate/bbrep

Suppression of MAGE-A10 alters the metastatic phenotype of tongue squamous cell carcinoma cells

Bruna dos Santos Mendonça[a], Michelle Agostini[b], Iara Gonçalves Aquino[b], Wagner Barbosa Dias[c], Débora Campanella Bastos[d], Franklin D. Rumjanek[a,*]

[a] Instituto de Bioquímica Médica Leopoldo de Meis, Centro de Ciências da Saúde, Universidade Federal do Rio de Janeiro Ilha do Fundão CEP 21941-902 Rio de Janeiro, Brazil
[b] Departamento de Patologia e Diagnóstico Oral - Faculdade de Odontologia, Universidade Federal do Rio de Janeiro, Brazil
[c] Laboratório de Glicobiologia Estrutural e Funcional Instituto de Biofísica-Universidade Federal do Rio de Janeiro, Rio de Janeiro, Brazil
[d] Faculdade de Odontologia de Piracicaba, Universidade Estadual de Campinas, Piracicaba, SP, Brazil

ARTICLE INFO

Keywords:
Mage-A10
Metastasis
Cytoskeleton
Migration
EMT

ABSTRACT

MAGE-A10 is a member of the MAGE protein family (melanoma associated antigen) which is overexpressed in cancer cells. Although MAGE-A10 has been characterized for some time and is generally associated to metastasis its function remains unknown. Here we describe experiments using as models oral squamous cell carcinoma (OSCC) cell lines displaying increasing metastatic potential (LN1 and LN2). These cell lines were transduced with lentivirus particles coding for short hairpin against MAGE-A10 mRNA. Repression of MAGE-A10 expression in LN2 cells altered their morphology and impaired growth of LN1 and LN2 cell lines. Furthermore, repression of MAGE-A10 expression increased cell-cell and cell matrix adhesion. Furthermore shMAGEA10 cells were shown to assemble aberrantly on a 3D culture system (microspheroids) when compared to cells transduced with the control scrambled construct. Cell migration was inhibited in knocked down cells as revealed by two different migration assays, wound healing and a phagokinetic track motility assay. In vitro invasion assay using a leiomyoma tissue derived matrix (myogel) showed that shMAGEA10 LN1 and shMAGEA10 LN2 cells displayed a significantly diminished ability to penetrate the matrices. Concomitantly, the expression of E-cadherin, N-cadherin and vimentin genes was analyzed. shMAGEA10 activated the expression of E-cadherin and repression N-cadherin and vimentin transcription.

Taken together the results indicate that MAGE-A10 exerts its effects at the level of the epithelial-mesenchymal transition (EMT) presumably by regulating the expression of adhesion molecules.

1. Introduction

Head and neck squamous cell carcinoma (HNSCC) is the sixth most common cancer worldwide [1,2], with a 5-year survival rate of 50% a value that remains relatively unchanged for the past three decades [3]. Tobacco exposure and alcohol consumption are responsible for the vast majority of HNSCC that occur in the oral cavity, larynx and hypo larynx [4]. The oral tongue squamous cell carcinoma (OTSCC) is the most common cancer in the oral cavity [5], characterized by a high incidence of metastasis to regional lymph nodes [6]. Besides, the local recurrence and second primary tumors also negatively impact the prognosis of patients with OTSCC who usually present significantly worse prognosis than those with squamous cell carcinomas of the oropharynx, larynx, hypo larynx and other oral cavity sites [7–9].

As a means to study the cellular processes associated to the progression of OTSCC we have resorted to a murine experimental model of three cell lines, SCC-9 derived from a primary human OTSCC, LN1 [10] and LN2 isolated from metastatic tumors of SCC-9 cells and which displayed increasing metastatic potential. The idea was to compare the phenotypes of the cell lines in order to gain insight into the process of metastatic progression and the cellular/biochemical mechanisms involved therein.

As a first line of enquiry, a non-targeted proteomic analysis was carried out in SCC-9, LN1 and LN2 cells (results not shown). Amongst the set of hundreds of proteins obtained, two of them stood out in terms of differential expression. These were identified as proteins of the MAGE family, MAGE-D2 in LN1 and LN2 cells and MAGE-A10 in LN2. The ratios of expression LN1/SCC-9 and LN2/SCC-9 were respectively

* Corresponding author.
E-mail addresses: bsmendonca@bioqmed.ufrj.br (B.d.S. Mendonça), michelleagostini@uol.com.br (M. Agostini), iaraa.aquino@hotmail.com (I.G. Aquino), wdias1976@gmail.com (W.B. Dias), bastosdc@hotmail.com (D.C. Bastos), franklin@bioqmed.ufrj.br (F.D. Rumjanek).

http://dx.doi.org/10.1016/j.bbrep.2017.04.009
Received 10 January 2017; Received in revised form 13 April 2017; Accepted 18 April 2017
Available online 19 April 2017

26 and 20 for MAGE-D2 and 62 for LN2/SCC-9.

The MAGE family gathers a large group of proteins which include a subset referred to as cancer/testis antigens (CTA) [11]. There are approximately 60 different members that have in common a 170 aminoacid homology domain [12]. Although the acronym MAGE stands for melanoma associated antigen, the proteins have been found to be expressed by many tumor types [13]. MAGE proteins are also highly expressed in proliferating germline cells [14]. Despite the fact that MAGEs are expressed in a wide-variety of cancers, both their transcriptional regulation and actual function within the oncogenic panorama remain fragmentary. Regarding the regulation of MAGE expression, results in the literature show that the demethylating agent 5-aza- 2-deoxycytidine can induce expression of MAGE-A1 suggesting that normally in somatic cells the expression of MAGEs is prevented by methylation of the promoter regions [15]. Concerning their oncogenic role it has been proposed that MAGEs can influence tumor progression by prompting the degradation of tumor suppressor factors through enhancement of ubiquitin ligase activity followed by degradation in the proteasome [16]. Other routes involving the MAGE dependent recruitment of p53 and its cognate targets have been put forward [17]. Even though it has not been possible to extend these individual findings to all members of the MAGE protein family a pattern is emerging that implicates MAGE proteins in the fine tuning of normal development during embryogenesis and gamete formation [18]. Hence it is reasonable to assume that deregulation of the MAGE dependent network can be a co-driver of tumorigenesis and particularly, metastasis. Despite the inherent complexity of metastasis, there is a consensus that cell–cell contact plays a central role [19,20]. One of the hallmarks of cancer is the detachment of cells from the primary tumor, followed by invasion and migration through the extracellular matrix, blood and lymphatic vessels and finally colonization of distant tissues [21–23]. The epithelial to mesenchymal transition (EMT), a developmental process in which epithelial cells lose polarity and develop a mesenchymal phenotype, has been implicated in the initiation of metastasis [24]. This process is characterized by loss of intercellular adhesion (E-cadherin and occludins); down-regulation of epithelial makers (cytokeratins); up-regulation of mesenchymal markers (Vimentin and N-cadherin); acquisition of fibroblast-like (spindle) morphology with cytoskeleton reorganization and increase in motility, invasiveness, and metastatic potential [20,22,24–27]. Recently, it was demonstrated that MAGE-A proteins were highly expressed at the tumor front of stage IV specimens compared with the tumor front of stage I specimens of head and neck squamous cell carcinoma [28]. Armed with this information it seemed plausible to narrow down the search for the function of MAGE-A10 protein by studying its participation in phenomena that are directly relevant to cell-cell interaction. Therefore, the top-down approach adopted in the present work aimed at investigating the effect of MAGE-A10 of LN1 and LN2 cells on parameters associated to morphology, migration, adhesion and invasion.

2. Materials and methods

2.1. Cells

SCC-9 cells stably expressing ZsGreen protein were implanted subcutaneously into the footpads of the left front limb of BALB/c nude mice and fragments of the metastatic axillary lymph nodes were used for explant cultures from which LN1 cell line was isolated [10]. Next LN1 cells were implanted subcutaneously into the footpads of other BALB/c nude mice and LN2 cells were isolated in the same way. When implanted into the tongue of BALB/c nude mice, LN1 metastasized to the cervical lymph nodes approximately 10 days after, in contrast to approximately 60 days consumed by the parental cells SCC-9. LN2 formed smaller primary tumors than LN1 cells, but metastasized even faster. Cells were cultured in Ham's F12 medium (DMEM/F12; Invitrogen, USA) supplemented with 10% fetal bovine serum (FBS), 400 ng/ml hydrocortisone (Sigma-Aldrich, USA) and the antibiotics penicillin and streptomycin. The cell lines were genotyped and tested for *Mycoplasma sp*. infection.

2.2. Suppression of MAGE- A10 expression

Specific suppression of human MAGE-A10 mRNA was achieved by transduction of lentiviral particles expressing oligonucleotides bearing a short hairpin structure (MISSION shRNA Lentiviral Transduction Particles, Sigma-Aldrich, USA). LN1 and LN2 cells grown in a 24-well plate at confluence of 50% were incubated with control or MAGE-A10 shRNA lentiviral particles. Cells were grown in culture media containing 8 μg/ml of polybrene (Sigma-Aldrich, USA) for 48 h. After washing with PBS, cells were cultured in fresh media for an additional period of 24 h. Cells were then diluted in a 1:5 suspension, and cultured for 10 days in the presence of 1 μg/ml of puromycin dihydrochloride (Sigma-Aldrich, USA) to select resistant cells (shMAGEA10). Control cells (shControl) were transduced with a scrambled construct. The efficacy of shMAGEA10 was determined by Real Time -qPCR and western blot assay with a hybridoma supernatant [29].

2.3. Cell morphology and circularity

Cell morphology was evaluated in an inverted microscope (Nikon Eclipse Ti-S) using the program ImageJ based on the formula $C = 4\pi \times [\text{area}][\text{Perimeter}]$ [30].

2.4. Cell proliferation index

Cells were initially cultivated in 24 well plates for 24 h, followed by 48 h in the absence of serum in order to induce synchronicity. Cells were then cultured for 24 and 48 h with fresh medium containing 10% fetal bovine serum (FBS), trypsinized and suspended in 1 ml of DMEM/F-12 supplemented with 10% FBS and counted in a Neubauer chamber. Cell viability was assayed using the trypan blue exclusion method.

2.5. Scratch (Wound Healing) assay

Cell migration was assayed by measuring the time required by cells to migrate into a “wound” produced on the surface of a confluent layer of cells [31]. For the assay, 24 well plates were used to grow the cells. Wounds were produced with a sterile disposable pipette tip. The medium was removed, the cells were washed with PBS and fresh medium without serum was added. Cells were incubated for 0, 3 and 6 h and were observed and photographed using a Nikon, Eclipse Ti fluorescence microscope. Observations from three different fields were used to plot the results in five independent experiments.

2.6. Phagokinetic track motility assay

In order to measure the motility of individual cells, cell migration was also estimated by the phagokinetic track motility assay using culture plates coated with colloidal gold [32]. Briefly, 500 cells LN1 and LN2 (shControl and shMAGEA10) were seeded onto gold sol-coated wells (24-well plates) and maintained at 37 °C in 5% CO_2 for 20 h. After incubation, the cells were observed and photographed using a light microscope. Motility track area of 15 cell/well were measured by ImageJ program and expressed as square pixels.

2.7. Transwell invasion with Myogel solidified with low-melting agarose (Myogel-LMA)

This assay was carried out as described by Salo et al., 2015 [33]. Briefly, 50 μL of the Myogel-LMA agarose mixtures was added on the upper chamber of Transwell® nylon filter membrane insert, incubated ½ h at room temperature and thereafter at 37 °C in a 5% CO_2

humidified atmosphere until the cells were ready to be seeded on the top of the gel. Cells were trypsinized and counted. 500 µL of 10% serum containing medium was added to the lower chamber of the Transwell®, and 50,000 cells were suspended in 100 µL of medium containing 0,5% BSA instead of serum and seeded onto the upper compartment of the Transwell® chamber. The cells were allowed to invade for two to three days. Invasion was quantified by staining the fixed cells (4% formaldehyde for 1 h at RT) with Toluidine Blue.

2.8. Adhesion assay

96-well culture plates were coated with 1 µg/µL of Matrigel® (BD Matrigel Matrix, BD Biosciences, Cat. Number 354234) in 100 µL of PBS for 24 h at 4 °C. At the same time, the cell culture medium was changed to serum-free medium. The wells were washed 3 times with 200 µL of PBS and then coated with the same volume of 3% bovine serum albumin (BSA) in PBS for 1 h at 37 °C. Control wells were coated only with 3% BSA solution. Cells were harvested and then resuspended in DMEM/F-12 supplemented with 3% BSA at a final concentration of 10,000 cells in 100 µL. The plates were then incubated for 2 h at 37 °C in 5% CO_2. Non-adherent cells were washed away and the remaining adhered cells were fixed with 10% formalin for 15 min and stained with 1% toluidine blue in 1% borax solution. Absorbance was measured at 650 nm.

2.9. Multicellular Tumor Spheroids (MCTS)

3D cell cultures were prepared essentially as described by Ho et al. [34]. Briefly, spheroids were produced by seeding U- bottom wells previously coated with 1% agarose with 2×10^4 cell suspended in 200 µL DMEM/F-12 medium containing 10% of FBS. With this setup cells do not adhere to the plastic matrix and are thus allowed to associate forming a multicellular 3D structure. The size of the aggregates was monitored every 24 h in the inverted microscope during a total of 72 h.

2.10. Real-time PCR

Total RNA from cell lines was extracted with the TRIzol® reagent (Invitrogen™), according to the manufacturer's protocols. Following DNase I treatment, 1 µg of total RNA per sample was used to generate cDNA using 1 U of DNAse I (Fermentas) and reverse transcriptase (High Capacity cDNA Reverse Transcription Kit – Applied Biosystems™). The resulting cDNAs were subjected to qPCR using specific primers. The sequences of the primers used are shown in Supplementary data table 1. and SYBR Green PCR master mix (Applied Biosystems,USA) in the 7500 Real Time PCR (Applied Biosystems, USA). Gene expression was determined using the delta-delta CT method and the housekeeping gene ACTB (beta-actin) was used as reference gene for data normalization. All reactions were performed in triplicate. Pairs of primers are described in S1 Table.

2.11. Whole cell protein extraction

Cells were grown to 70% washed with cold PBS and then lysed manually for 3 min with a Wheaton Potter-Elvehjem homogenizer in an ice bath in RIPA buffer containing 50 mM de TRIS-HCl pH 8,0, 150 mM sodium chloride, 1% NP-40, 0,5% sodium deoxycholate, 0,1% sodium dodecyl sulphate (SDS) supplemented with the protease inhibitors 1 mM phenyl methylsulfonylfluoride (PMSF) and CIP (Sigma-Aldrich® – P8340) at a proportion of 1 µL of CIP for every 100 µL of extraction buffer. The extract was then transferred to a 1.5 ml microcentrifuge tube and centrifuged at 1000*g* for 5 min in order to discard cell debris.

2.12. Western blot

30 µg of total proteins per sample were fractionated in a 12% SDS-PAGE using a running buffer containing 125 mM de TRIS base, 1.25 M glycine and 0,5% de SDS (w/v) during approximately 2 h at 120 V under reducing conditions, and transferred to nitrocellulose membranes (Bio Rad Trans-Blot Turbo Midi-size nitrocellulose) in a buffer solution consisting of 39 mM glycine, 48 mM TRIS-base, 0037% SDS (p/v) and 20% (V/V) methanol (BIO-RAD- Trans-Blot Turbo 5x Transfer Buffer). Protein fractionation and transfer were carried out in a Mini-Protean II system (BIO-RAD). After transfer the membranes were blocked with Odyssey blocking buffer according to the manufacturer's instructions and subsequently incubated for up to 24 h with the primary antibodies (S2 Table). Monoclonal antibody mAb 3GA11 (MAGE-A10) used as a primary antibody was a kind gift by Dr. Giulio C. Spagnoli from the Department of Surgery, Research Laboratory, University Hospital Basel, Basel, Switzerland. The secondary antibody was IRDye 800CW goat anti-mouse immunoglobulin. Bands were visualized in a Li-Cor Odyssey western blot imaging system.

2.13. Protein assay

Proteins were quantified using the Bio-Rad Protein Assay, Bio-Rad, USA.

3. Results

3.1. MAGE-A10 is overexpressed in tongue squamous metastatic cells

Gene expression MAGE-A10 transcripts is clearly higher in LN1 and

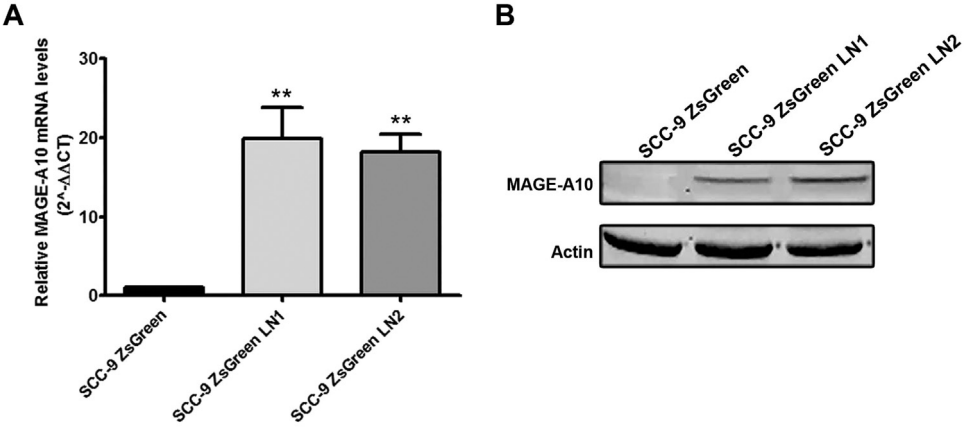

Fig. 1. MAGE-A10 is overexpressed in tongue squamous cells. (A) MAGEA10 mRNA levels assayed by RT-qPCR in SCC-9, LN-1 and LN-2 cell lines. (B) Western blot of MAGE-A10 protein levels. Values of 2^ΔΔCT were normalized by β-actin levels and are expressed in relation to SCC-9 levels. Bars represent the means ± SEM of three independent experiments. $^{**}p > 0.01$.

LN2 cells than in the parental SCC-9 cells as shown by the results in Fig. 1A using RT-qPCR. This result actually validates the RNA-seq whole transcriptome sequencing analysis of LN1 and LN2 cells, which originally showed a dramatic overexpression of MAGE proteins reported for other metastatic tumors [35,36] The Ct values For SCC-9 cells for SCC9 cells were in the range 28–30, whereas these were 22–25 for LN1 and LN2 cells.

The relative high level of MAGE-A10 transcription was paralleled by protein abundance as shown by the western blot analysis depicted in Fig. 1B. Although in LN2 cells the MAGE-A10 band is slightly more intense than that to LN1 cells, it is clear that the amounts of MAGE-A10 in both cell lines are comparable and decidedly much higher than the parental SCC-9 cells.

However, it must be borne in mind that high transcription rates are not necessarily paralleled by high translation rates [37].

3.2. Depletion of MAGE-A10 affects cell morphology, growth, adhesion and invasion

To examine the role of MAGE-A10 in oral metastatic cancer cells, we suppressed MAGE-A10 expression in LN1 and LN2 cell lines, using the short hairpin approach. The silenced cells were referred to as: shMAGEA10 LN1 or LN2. After puromycin selection, stable transfectants were obtained. Attempts to produce knocked down cells for MAGE-A10 generated 5 clones. Among these, two exhibited constitutively reduced levels of MAGE-A10 mRNAs in relation to the cells transduced with the scrambled control constructs (Supplementary Fig. 1). Based on these results the silenced clones (#2 and #4) were then used indistinctively in all subsequent experiments. RT-qPCR and immunoblot analyses indicated that MAGE-A10 expression was significantly decreased in all shMAGEA10 cells compared with shControl cells (Fig. 2A, B and C).

Firstly we examined whether in monolayer cell cultures shMAGE-A10 cells displayed observable gross morphological differences. The results in Fig. 2D and E addressed this issue. The results in Fig. 2D highlight the following features: LN1 shControl cells and LN1 shMAGEA10 exhibited fusiform cell bodies bearing cytoplasmic extensions. Both tended to form heterogeneous cultures with little intercellular space. In contrast, LN2 shMAGEA10 cells were rounder when compared to the LN2 shControl cells, which were less spindle-like in shape and fibroblastic, and the pseudopods were shorter than those of control cells; also cells tended to associate forming bigger clusters in culture.

The differences between the cell clones became clearer when circularity was measured, as shown in Fig. 2E. These results show that with respect to morphology the more pronounced effect of silencing MAGE-A10 was clearly manifest in LN2 cells. On the other hand shMAGE-A10 affected both cell lines in terms of proliferation as shown in Fig. 2F. Interestingly, inhibition of proliferation was more pronounced at 24 h, particularly in LN2 cells.

Similar experiments were carried out in order to evaluate the effect of shMAGE-A10 on the architecture of MCTS. The results in Fig. 2G show that LN1 and LN2 cells transduced with the shControl construct and left to grow for 24–72 h generated cell aggregates that were considerably looser than their knocked down counterparts (#2 and #4), indicating that shMAGEA10 cells displayed a tighter association between cells. That MAGE-A10 was involved in cell-cell adhesion was also suggested by the observation that shControl cells could be easily dissociated mechanically, whereas LN1 shMAGEA10#2 and LN1 shMAGEA10#4 required trypsin treatment for dissociation to occur (results not shown).

The effect of shMAGE-A10 on cell-cell adhesion was even more striking when LN2 cells were compared. LN2 shControl were unable to aggregate tightly even at 72 h, whereas LN2 shMAGEA10#2 and LN2 shMAGEA10#4 maintained the compact spherical cell aggregates at all times. In order to evaluate the effect of suppressing MAGE-A10 on MCTS, the circularity index of the cell aggregates was calculated. The results are shown in Fig. 2H. Although circularity did not inform about cell-cell adhesion it certainly highlighted the fact that in both cell lines, shControl and shMAGEA10 cells formed two distinct populations. The populations consisting of LN1 and LN2 shControl were significantly less able to form spheroid than their suppressed counterparts. Consistently, matrigel adhesion assays showed that only LN2 shMAGEA10 cells displayed higher adherence to the matrix as shown in Fig. 2I.

Because the effects observed so far suggested the possible involvement of cytoskeleton proteins involved in cell motility - actin filaments, myosin II and intermediate filaments - the next set of experiments focused on cell migration. To that end, we first compared the cell motility and migration of the cell lines, as determined by haptotaxis on colloidal gold plates and the scratch assay, respectively. Both shMAGEA10 cells showed a marked reduction in cell motility and migration. The results are shown in Fig. 3A–D. The results in Fig. 3A shows the paths of cell migration estimated by the tracks left on the plate as a consequence of phagocytosis of the colloidal gold. Fig. 3B shows the plots of the areas corresponding to the migration. Presumably, in the case of the phagokinetic track motility assay, the phagocytic process itself might have been compromised since migration and phagocytosis might share cytoskeleton proteins. Control and shMAGEA10 cells were also analyzed on a scratch assay. Again, we observed that silencing of MAGE-A10 affected the migration of both cells lines. By quantifying the migration (Fig. 3D) it can be seen that the effect of shMAGE A10 was quite visible after 6 h and that the migration of LN1 shMAGEA10 and LN2 shMAGEA10 were inhibited to the same extent.

Along the same line of reasoning, we carried out invasion assays since the migration of metastatic cells followed by colonization is bound to rely on processes associated to the cytoskeleton, actin polymerization and myosin motor proteins. Fig. 4A shows photographs of toluidine blue staining of control and shMAGE-A10 cells in Transwell/Myogel-LMA assay after 48 and 72 h incubation. The plot in Fig. 4B cells represents the absorbance of extracted toluidine blue from LN1 and LN2 cells that penetrated the Myogel and Transwell insert. Invasion of LN1 shMAGEA10 cells was significantly reduced at 48 h. However, inhibition of invasion was more pronounced when LN2 shMAGEA10 cells at 48 and 72 h. The behavior of shMAGEA10 LN2 cells in the invasion assay is in keeping with those seen in Fig. 2D and E and is consistent with the gradient of invasive potential that exists between LN1 and LN2 cells.

3.3. MAGE-A10 regulates genes associated with EMT

Finally we asked whether the expression of the adherens junction's proteins E-cadherin and N-cadherin, was affected by the silencing of MAGE-A10 in LN cells. These proteins are generally considered to be markers of Epithelial to Mesenchymal Transition (EMT). EMT is a dynamic, reversible event that governs cell migration during normal tissue repair and development and that becomes severely disrupted during malignant transformation [23–27]. The results are shown in Fig. 5A-C. LN1 shMAGE-A10 cells expressed E-cadherin mRNA almost twice as much as the control cells (Fig. 5A). Similar values for overexpression of E-cadherin were recorded for LN2 shMAGE-A10 cells (Fig. 5B). In contrast, N-cadherin expression was inhibited in both cell lines. Furthermore, the expression of type III intermediate filament protein vimentin, a major component of the cytoskeleton of mesenchymal cells, was also reduced as a result of shMAGE-A10. The results in Fig. 5C are western blots that reproduce MAGE-A10 effect on gene expression, that is, increase in E-cadherin and a reduction of N-cadherin and vimentin protein synthesis. The MAGE-A10 dependent enhancement of E-cadherin and the concomitant suppression of N-cadherin and vimentin suggest that MAGE-A10 does indeed have a role in EMT, possibly by interfering with cytoskeleton elements that under normal circumstances would impair cell-cell dissociation.

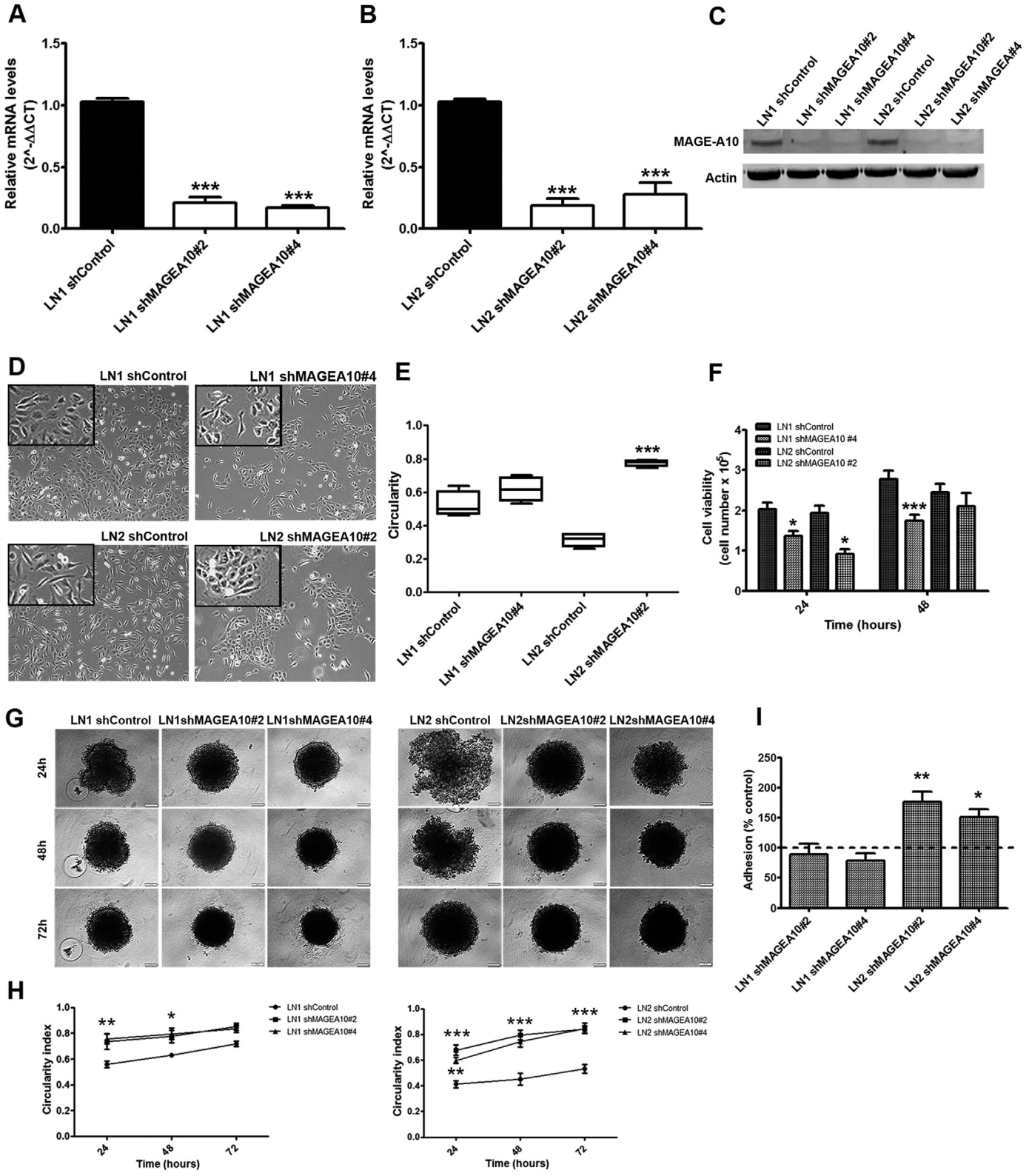

Fig. 2. shMAGEA10 exhibits altered cell viability, morphology, growth and adhesion. (A-B) RT-qPCR analysis of MAGE-A10 expression in LN1 and LN2 cells stably expressing shMAGEA10 (#2 and #4), and shControl cells displaying puromycin resistance after transduction. (C) Immunoblot of cell lysates of shMAGEA10 and shControl showing the suppression efficiency of MAGE-A10 protein expression. (D) Trypan blue exclusion cell viability analysis. (E) Morphology analysis of shMAGEA10 and shControl cells observed at magnification 10x. (F) Cell circularity plots calculated using ImageJ software by the formula $C = 4\pi \times [Area]/[Perimeter]^2$. (G) Spheroid formation assay performed in 24, 48 and 72 h. (H) Spheroid circularity index calculated by ImageJ software. The graphs represent analyses of the spheroid circularity of LN1 and LN2 cells, controls and silenced. $^*p < 0.05$, $^{**}p < 0.01$, $^{***}p < 0.001$.

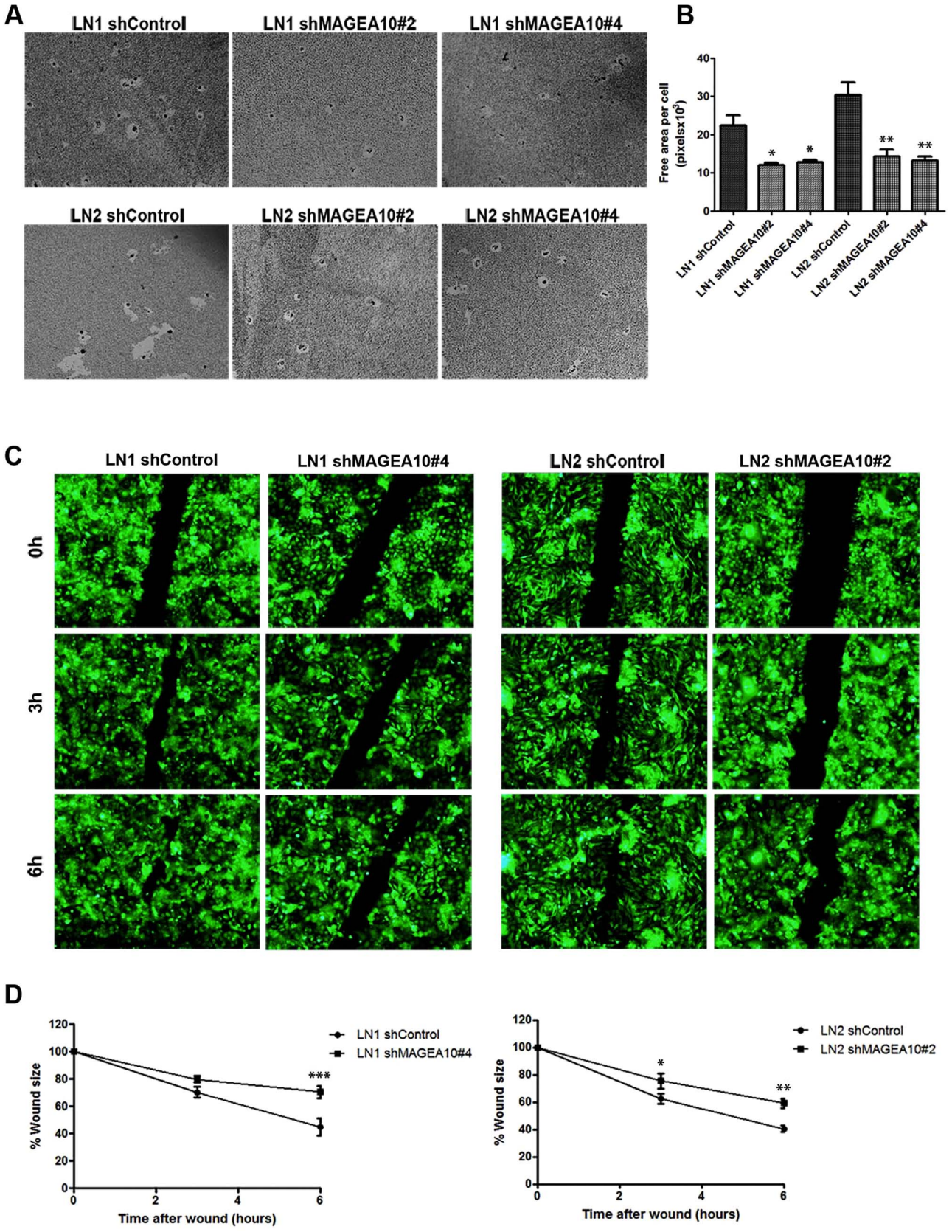

Fig. 3. shMAGE-A10 affects single cell motility and migration. (A-B): cell motility was quantified by measuring the track area free of gold nanoparticles after 24 h. Motility was estimated by measuring the areas of 10 cells/well using ImageJ software and were expressed in pixels. The graphs represent the mean track area of the LN1 and LN2 control and shMAGEA10 cell lines (C-D): migration of LN1 and LN2 cells (shMAGEA10 or shControl) was assessed using the Wound Healing assay. Images were taken at times 0, 3 and 6 h under a fluorescence microscope. The graphs represent the quantification of scratch spaces over time. The values were normalized with respect to time 0 h and represent mean ± standard error.

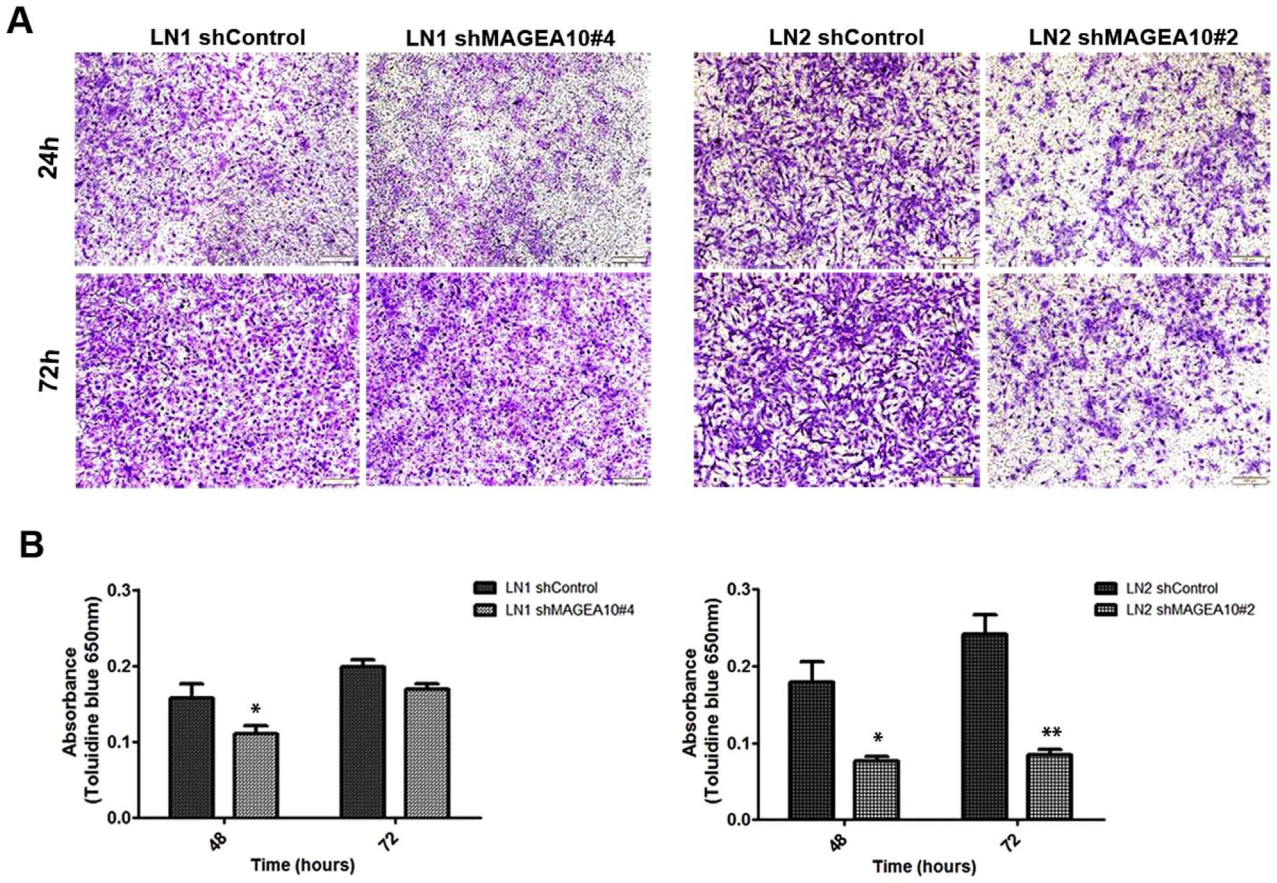

Fig. 4. shMAGE-A10 cells showed a significant reduction of cell invasion. The ability to invade and degrade the matrix by LN1 and LN2 cells (shMAGEA10 or shControl) was determined by the Myogel invasion assay. (A): LN1 shControl and shMAGEA10 and LN2 shControl and LN2 shMAGEA10, respectively. Illustrative images of the LN1 and LN2 cells control and shMAGEA10 that invaded and crossed into the transwell (magnification 10x). (B): plot quantifying toluidine blue stained cells in the Myogel matrix by absorbance at 650 nm $*p < 0.05$; $**p < 0.01$; $***p < 0.001$.

4. Discussion

The fact that proteins of the MAGE family are found to be highly expressed in proliferating germline cells and malignant cells alike indicate that functionally they must occupy prominent positions in regulatory pathways that normally control cell growth and movement [38]. Supposedly, rather than any structural changes that would imply gain of function, it is the untimely, continuous overexpression of MAGE proteins that characterizes their subversive role sustaining oncogenic behavior. However, there is not much information regarding the dysregulation of MAGE protein biosynthesis, apart from reports showing that demethylating agents can induce the expression of some members of the MAGE protein family [15]. Likewise for the mode of action of these proteins. Presumably, the relative scarcity of biochemical data about MAGE proteins may have resulted from the earlier emphasis of research on immunotherapy as a means to control tumor progression [39]. Notwithstanding, the overexpression of MAGE proteins in certain cancers suggests its participation in central processes associated to malignancy, among which those that involve cell-cell adhesion [40–43]. Collectively the results reported in the present work showed that the function of MAGE-A10 proteins which are over expressed in squamous cell carcinoma, may be narrowed down to cell-cell interaction, cell deformability and cell motility. These conclusions were derived from experiments showing that shMAGEA10 LN1

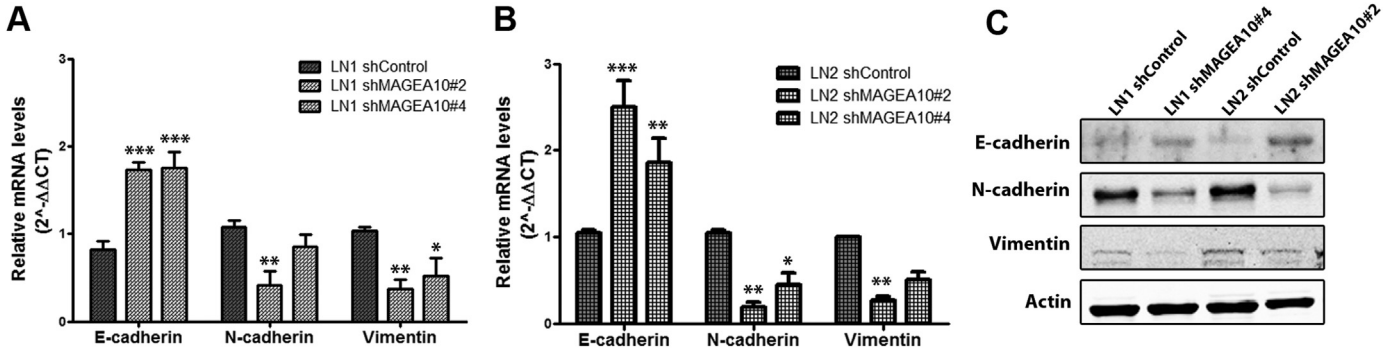

Fig. 5. shMAGEA10 cells display an altered EMT phenotype in tongue squamous metastatic cells. (A-B) RT-qPCR analysis of epithelial and mesenchymal markers. (C) Immunoblot analysis of epithelial and mesenchymal markers. The values were loaded normalized by β-actin levels and were expressed relatively to control levels. $*p < 0.05$; $**p < 0.01$; $***p < 0.001$.

and shMAGEA10 LN2 cells showed alterations of cell morphology and of parameters associated with migration, and invasion. Likewise in those cells the expression of proteins that are consensually accepted as being markers of EMT were modulated. The results described in Fig. 2G and I illustrate this point quite clearly. In the more aggressive LN2 cells, a reduction of MAGE-A10 production increased the adherence of LN2 cells to each other in the spheroid model and to matrigel in the adhesion assay, respectively. Thus, considering the in vivo situation, the overexpression of MAGE-A10 would assist metastasis by facilitating cell-cell deadhesion. A possible mechanistic interpretation is that MAGE-A10 may directly block cell-cell interaction by interfering with proteins that would normally mediate cell attachment. Vimentin, for example. This protein whose initial role was believed to be restricted to mechanical stabilization of cells is now known to promote cell adhesion, motility and participate in signaling networks thanks to its association with several different proteins [44]. Consistently, the results of Figs. 3A-D and 4 indicate that the effect of MAGE-A10 could be two-pronged, i.e. blocking the action of vimentin at the same time it inhibits its *de novo* synthesis. The results in Fig. 3E and F also show that MAGE-A10 was implicated in invasion, since its suppression affected this process. Even though the colonization of distant tissues by metastatic cells is a multistep process, involving not only migration, any interference with the motile elements of the cytoskeleton may be enough to impair invasion [24].

Naturally, the results reported here do not exclude the participation of other proteins as targets for MAGE-A10 such as catenins that act by connecting cadherins to the cytoskeleton, as well as to other signaling pathways. In this respect, complex processes such as those involved in cell migration do require an array of proteins such as actin, myosin II, keratins, integrins, vinculin, cofilin and others that by interacting in a concerted way coordinate the machinery underlying cell motility and intracellular trafficking [45]. In addition the same proteins acting individually or in association may respond to MAGE-A10 over expression by interfering with transmembrane adhesion molecules and other components of the cytoskeleton capable of transmitting signals across the plasma membrane that can also propagate into the cytoplasm and nucleus. Keratins are a case in point. The non-targeted proteome of LN1 and LN2 cells has revealed that a number of non-hair keratin variants are overexpressed in both cell lines (unpublished results). Although the physiopathology associated to keratins is not entirely clear, their expression is frequently used for determining the epithelial origin of several types of cancer, including oral squamous cell carcinoma [46]. Because of its intracellular location and association with integrins, one could propose a role for keratins as intracellular sensors transducing and communicating extracellular signals derived from the interaction between cells. In this context MAGE-A10 could also be considered a ligand of keratins, thus ultimately enabling cells to detach from the primary tumor, acquire resistance to anoikis and migrate to distant sites. Although early reports have located MAGE-1 in the cytosol of melanoma cells [47], this finding cannot be generalized to the whole protein family. At any rate, the potential role of MAGE-A10 as a mediator of cell deadhesion would require it to display high connectivity with other members of signaling pathways. Although this has not yet been investigated within the context of wet laboratory experiments, interesting *in silico* approaches have revealed that proteins of the MAGE family are essentially disordered with regards to their secondary structure [48]. Proteins falling into that category contain in their structures the so called intrinsically disordered domains, regions that lack a stable three-dimensional structure under physiological conditions. Because of that proteins bearing disordered domains are endowed with functional versatility since they can interact with many different ligands [49]. A high degree of plasticity with regards to protein-protein interaction is in fact a hallmark of most hub proteins. For example, HIF-1α or p53 and other transcription factors that occupy central positions in signaling pathways are indeed composed of many repetitive structural domains and relatively long stretches of intrinsically disordered regions (IDRs) [50]. Or, put another way, proteins can only behave as hubs because they contain IDRs. Because MAGE-A10 protein does contain intrinsically disordered domains it could be predicted that it would display a high degree of allostery compatible with the mediation of multiple interactions. The interactions of such structurally dynamic proteins would be of a transient nature dictated by low affinity binding to the different ligands. Plausibly, the observed overexpression of MAGE-A10 in LN1 and LN2 cells may reflect a situation in which increased quantities of the protein might compensate for the implied IDR-related low affinity binding. Viewed as such one could hypothesize that the equilibrium of cell adhesion-deadhesion is a consequence of MAGE-A10 repression or synthesis. In tumors the chronic overexpression of MAGE-A10 would shift the equilibrium towards cell-cell deadhesion and could thus be regarded as one of the promoters of the metastatic process.

Acknowledgements

The authors wish to acknowledge Dr. Giulio C. Spagnoli from the Department of Surgery, Research Laboratory, University Hospital Basel, Basel, Switzerland for the kind gift of the monoclonal antibody mAb 3GA11 (MAGE-A10) used as a primary antibody and the financial support of CNPq (304106/2014-3), INCT Controle do Câncer (573806/2008-0), Faperj (E-26/201.251/2014), CAPES-COFECUB (2528/2014) and Fundação do Câncer.

Appendix A. Transparency document

Transparency document associated with this article can be found in the online version at http://dx.doi.org/10.1016/j.bbrep.2017.04.009.

References

[1] A.C. Chi, T.A. Day, B.W. Neville, Oral cavity and oropharyngeal squamous cell carcinoma- an update, CA Cancer J. Clin. 5 (2015) 401–421.
[2] E.P. Simard, L.A. Torre, A. Jemal, International trends in head and neck cancer incidence rates: differences by country, sex and anatomic site, Oral Oncol. 50 (2014) 387–403.
[3] A. Jemal, R. Siegel, E. Ward, Y. Hao, J. Xu, M.J. Thun, Cancer statistics, 2009, CA Cancer J. Clin. 9 (2009) 225–249.
[4] S.I. Pai, W.H. Westra, Molecular pathology of head and neck cancer: implications for diagnosis, prognosis, and treatment, Annu. Rev. Pathol. 4 (2009) 49–70.
[5] M.L. Durr, A. van Zante, D. Li, E.J. Kezirian, S.J. Wang, Oral tongue squamous cell carcinoma in never-smokers analysis of clinicopathologic characteristics and survival, Otolaryngol. Head. Neck Surg. 149 (2013) 89–96.
[6] D. Sano, J.N. Myers, Metastasis of squamous cell carcinoma of the oral tongue, Cancer Metastas. Rev. 26 (2007) 645–662.
[7] K. Rusthoven, A. Ballonoff, D. Raben, C. Chen, Poor prognosis in patients with stage I and II oral tongue squamous cell carcinoma, Cancer 112 (2008) 345–351.
[8] I.O. Bello, Y. Soini, T. Salo, Prognostic evaluation of oral tongue cancer: means, markers and perspectives (I), Oral. Oncol. 46 (2010) 630–635.
[9] A.V. Priante, E.C. Castilho, L.P. Kowalski, Second primary tumors in patients with head and neck cancer, Curr. Oncol. Rep. 13 (2011) 132–137.
[10] M. Agostini, L.Y. Almeida, D.C. Bastos, R.M. Ortega, F.S. Moreira, F. Seguin, et al., The fatty acid synthase inhibitor orlistat reduces the growth and metastasis of orthotopic tongue oral squamous cell carcinomas, Mol. Cancer Ther. 13 (2014) 585–595.
[11] J.L. Weon, P.R. Potts, The MAGE protein family and cancer, Curr. Opin. Cell Biol. 37 (2015) 1–8.
[12] P. Chomez, O. De Backer, M. Bertrand, E. De Plaen, T. Boon, S. Lucas, An overview of the MAGE gene family with the identification of all human members of the family, Cancer Res 61 (2001) 5544–5551.
[13] A.A. Jungbluth, S. Ely, M. DiLiberto, R. Niesvizky, B. Williamson, D. Frosina, et al., The cancer-testis antigens CT7 (MAGE-C1) and MAGE-A3/6 are commonly expressed in multiple myeloma and correlate with plasma cell proliferation, Blood 106 (2005) 167–174.
[14] M.J. Scanlan, A.J. Simpson, L.J. Old, The cancer/testis genes: review, standardization, and commentary, Cancer Immun. 4 (2004) 1.
[15] H.H. Cheung, Y. Yang, T.L. Lee, O. Rennert, W.Y. Chan, Hypermethylation of genes in testicular embryomal carcinomas, Br. J. Cancer 114 (2016) 230–236.
[16] J. Hao, R. Shen, Y. Li, Y. Zhang, Y. Yin, Cancer-testis antigen HCA587/MAGE-C2 interacts with BS69 and promotes its degradation in the ubiquitin-proteasome pathway, Biochem. Biophys. Res. Commun. 449 (2014) 386–391.
[17] M. Monte, M. Simonatto, L.Y. Peche, D.R. Bublik, S. Gobessi, M.A. Pierotti, et al., MAGE-A tumor antigens target p53 transactivation function through histone

deacetylase recruitment and confer resistance to chemotherapeutic agents, Proc. Natl. Acad. Sci. USA 103 (2006) 11160–11165.
[18] L.J. Old, Cancer is a somatic cell pregnancy, Cancer Immun. 7 (2007) 19.
[19] D. Hanahan, R.A. Weinberg, Hallmarks of cancer: the next generation, Cell 144 (2011) 646–674.
[20] M.A. Nieto, The ins and outs of the epithelial to mesenchymal transition in health and disease, Annu. Rev. Cell Dev. Biol. 27 (2011) 347–376.
[21] X. Guan, Cancer metastases: challenges and opportunities, Acta Pharm. Sin. B 5 (2015) 402–418.
[22] G.P. Gupta, J. Massague, Cancer metastasis: building a framework, Cell 127 (2006) 679–695.
[23] P. Savagner, Leaving the neighborhood: molecular mechanisms involved during epithelial–mesenchymal transition, Bioessays 23 (2001) 912–923.
[24] J.P. Thiery, Epithelial–mesenchymal transitions in tumour progression, Nat. Rev. Cancer 2 (2002) 442–454.
[25] E.W. Thompson, D.F. Newgreen, D. Tarin, Carcinoma invasion and metastasis: a role for epithelial–mesenchymal transition? Cancer Res. 65 (2005) 5991–5995.
[26] J.P. Thiery, J.P. Sleeman, Complex networks orchestrate epithelial– mesenchymal transitions, Nat. Rev. Mol. Cell Biol. 7 (2006) 131–142.
[27] J.P. Thiery, H. Acloque, R.Y. Huang, M.A. Nieto, Epithelial–mesenchymal transitions in development and disease, Cell 139 (2009) 871–890.
[28] S. Hartmann, M. Brisam, S. Rauthe, O. Driemel, R.C. Brands, A. Rosenwald, et al., Contrary melanoma-associated antigen-A expression at the tumor front and center: a comparative analysis of stage I and IV head and neck squamous cell carcinoma, Oncol. Lett. 12 (2016) 2942–2947.
[29] E. Schultz-Thater, S. Piscuoglio, G. Iezzi, C. Le Magnen, P. Zajac, V. Carafa, L. Terracciano, et al., MAGE-A10 is a nuclear protein frequently expressed in high percentages of tumor cells in lung, skin and urothelial malignancies, Int. J. Cancer 129 (2011) (2011) 1137–1148.
[30] M.H. Zaman, L.M. Trapani, A.L. Sieminski, D. Mackellar, H. Gong, R.D. Kamm, et al., Migration of tumor cells in 3D matrices is governed by matrix stiffness along with cell-matrix adhesion and proteolysis, Proc. Natl. Acad. Sci. USA 103 (2006) 10889-–110894.
[31] C.C. Liang, A.Y. Park, J.L. Guan, *In vitro* scratch assay: a convenient and inexpensive method for analysis of cell migration in vitro, Nat. Protoc. 2 (2007) 329–333.
[32] M.T. Nogalski, G.C. Chan, E.V. Stevenson, D.K. Collins-McMillen, A.D. Yurochko, A quantitative evaluation of cell migration by the phagokinetic track motility assay, J. Vis. Exp. 70 (2012) e4165.
[33] T. Salo, M. Sutinen, E. Hoque Apu, E. Sundquist, N.K. Cervigne, C.E. de Oliveira, et al., A novel human leiomyoma tissue derived matrix for cell culture studies, BMC Cancer 15 (2015) 981.
[34] W.Y. Ho, S.K. Yeap, C.L. Ho, R.A. Rahim, N.B. Alitheen, Development of multi-cellular tumor spheroid (MCTS) culture from breast cancer cell and a high throughput screening method using the MTT assay, PLoS One 7 (2012) e44640.
[35] B.J. van den Eynde, P.T. van der Bruggen, Cell defined tumor antigens, Curr. Opin. Immunol. 9 (1997) 684–693.
[36] J. Lin, L. Lin, D.G. Thomas, G.S. Greenson, T.J. Giordano, G.S. Robinson, et al., Melanoma-associated antigens in esophageal adenocarcinoma, Clin. Cancer Res. 10 (2004) 5708–5716.
[37] R. Moreno-Sanchez, E. Saavedra, J.C. Gallardo-Perez, F.D. Rumjanek, S. Rodriguez-Enriquez, Understanding the cancer cell phenotype beyond the limitations of current omics analyses, FEBS J. 283 (2016) 54-–573.
[38] M.H. Gjerstorff, M.H. Andersen, H.J. Ditzel, Oncogenic cancer/testis antigens: prime candidates for immunotherapy, Oncotarget 6 (2015) 15772–15787.
[39] D.W. Meek, L. Marcar, MAGE-A antigens as targets in tumour therapy, Cancer Lett. 324 (2012) 126–132.
[40] W. Liu, S. Cheng, S.L. Asa, S. Ezzat, The melanoma associated antigen A3 mediates fibronectin-controlled cancer progression and metastasis, Cancer Res. 68 (2008) 8104–8112.
[41] T. Suyama, T. Shiraishi, Y. Zeng, W. Yu, N. Parekh, R.L. Vessella, et al., Expression of cancer/testis antigens in prostate cancer is associated with disease progression, Prostate 70 (2010) 1778–1787.
[42] A.A. Jungbluth, S. Ely, M. DiLiberto, R. Niesvizky, B. Williamson, D. Frosina, et al., The cancer-testis antigens CT7 (MAGE-C1) and MAGE-A3/6 are commonly expressed in multiple myeloma and correlate with plasma cell proliferation, Blood 106 (2005) 0167–0174.
[43] B. Yang, S. O'Herrin, J. Wu, S. Reagan-Shaw, Y. Ma, M. Nihal, et al., Select cancer testis antigens of the MAGE-A, -B, and -C families are expressed in mast cell lines and promote cell viability in vitro and in vivo, J. Investig. Dermatol. 127 (2007) 267–275.
[44] J.M. Dave, K.J. Bayless, Vimentin as an integral regulator of cell adhesion and endothelial sprouting, Microcirculation 21 (2014) 333–344.
[45] J. Miyoshi, Y. Takai, Structural and functional associations of apical junctions with cytoskeleton, Biochim. Biophys. Acta 2008 (1778) 670–691.
[46] D.M. Toivola, P. Boor, C. Alam, P. Strnad, Keratins in health and disease, Curr. Opin. Cell Biol. 32 (2015) 73-–781.
[47] A. Amar-Costesec, D. Godelaine, E. Stockert, P. van der Bruggen, H. Beaufay, Y.T. Chen, The tumor protein MAGE-1 is located in the cytosol of human melanoma cells, Biochem Biophys. Res Commun. 204 (1994) 710–715.
[48] K. Rajagopalan, S.M. Mooney, N. Parekh, R.H. Getzenberg, P. Kulkarni, A majority of the cancer/testis antigens are intrinsically disordered proteins, J. Cell Biochem. 112 (2011) 3256–3267.
[49] P.E. Wright, H.J. Dyson, Intrinsically disordered proteins in cellular signalling and regulation, Nat. Rev. Mol. Cell Biol. 16 (2015) 18–29.
[50] M. Ota, H. Gonja, R. Koike, S. Fukuchi, Multiple-localization and hub proteins, PLoS One 11 (2016) e0156455.